Journal of Rock Mechanics and Geotechnical Engineering 12 (2020) 1093–1102

Contents lists available at ScienceDirect

Journal of Rock Mechanics and Geotechnical Engineering

journal homepage: www.jrmge.cn

Full Length Article

Effect of biopolymers on permeability of sand-bentonite mixtures

M.S. Biju, D.N. Arnepalli*

Department of Civil Engineering, Indian Institute of Technology Madras, Chennai, 600036, India

ARTICLE INFO

Article history:
Received 20 August 2019
Received in revised form
10 January 2020
Accepted 23 February 2020
Available online 31 July 2020

Keywords:
Geotechnical centrifuge
Landfill liner
Synthetic leachate
Xanthan gum
Guar gum

ABSTRACT

Application of biopolymer-modified geomaterials in waste disposal practices is gaining wide acceptance due to their superior tensile characteristics and improved crack resistance. Permeability is an important design parameter which determines the suitability of a material as a liner for construction of engineered landfills. Given this, the permeability characteristics of sand-bentonite mixtures amended with biopolymers was studied using a modified-falling head permeability apparatus under an accelerated gravity environment. Both distilled water and synthetic leachate were utilized as permeant liquid to assess the role of biopolymer amendment on the permeation behavior of sand-bentonite mixtures. Experimental results indicate that addition of biopolymers causes aggregation of the clay platelets, which in turn enhances the permeation behavior of the biopolymer-modified sand-bentonite mixtures. These mixtures meet the regulatory requirement of the liner.

1. Introduction

The effectiveness of sand-bentonite mixtures (SBMs) as barriers in the construction of waste disposal facilities is a proven fact (Sobti and Singh, 2017). Permeability is the critical property that determines the suitability of SBM as a liner. The presence of cracks in a barrier having sufficiently low permeability may fail to perform its intended purpose. A cover liner of an engineered landfill is subjected to cracking due to differential settlements, desiccation, and distress in the slope. For this, various remedial methods have been proposed to mitigate crack initiation and propagation in compacted clay barriers. Researchers have investigated the effects of various soil amendment techniques involving cement and fly ash, and inclusion of materials like polypropylene, glass, softwood pulp and polyester fibers to the soil matrix, for enhancing the liner performance (e.g. Adaska, 1985; Maher and Ho, 1994; Chaduvula et al., 2017; Thyagaraj and Soujanya, 2017). Considering the adverse environmental impacts of traditional additives, the feasibility of biopolymer application for improving the engineering performance of the geomaterials is also reported (e.g. Biju and Arnepalli, 2019). Favorable modifications of strength, dispersivity, erosion resistance, permeability, and swell-shrink of soils, upon amendment of these materials by biopolymers, have been reported in the literature (Khachatoorian et al., 2003; Bouazza et al., 2009; Chang et al., 2016; Acharya et al., 2017; Ayeldeen et al., 2017; Cabalar et al., 2017; Latifi et al., 2017; Dehghan et al., 2018; Ikeagwuani and Nwonu, 2019). In general, stabilization of the geomaterials using a variety of additives has resulted in improved crack resistance and tensile strength behaviors of geomaterials; however, these additives have posed a detrimental effect in terms of increased permeability (Maher and Ho, 1994; Abdi et al., 2008; Mukherjee and Mishra, 2017; Thyagaraj and Soujanya, 2017). Though many studies have been made on the application of biopolymers for stabilization of geomaterials, assessing their influences on the permeability behavior of SBMs is rarely reported.

The majority of the regulatory authorities suggest that the coefficient of permeability of a landfill liner shall be less than 1×10^{-9} m/s. Permeability measurement of such low permeable materials using a flexible wall permeameter requires a long testing duration (Anderson et al., 2015). Further, the presence of microorganisms in permeant liquid and porous media may induce clogging, which in turn yields erroneous results when testing periods are long. On the contrary, the coefficient of permeability of SBMs obtained indirectly from consolidation data yields low values compared to that obtained as per ASTM D5084-16a (2016) using a flexible wall permeameter (Gueddouda et al., 2016). In this regard, researchers have conducted falling-head permeability test in an accelerated gravity environment using a geotechnical centrifuge to reduce the test duration (Singh and Gupta, 2000; Singh and Kuriyan, 2002; Taylor, 2005; Timms et al., 2016). Over

* Corresponding author.
E-mail address: arnepalli@iitm.ac.in (D.N. Arnepalli).

Peer review under responsibility of Institute of Rock and Soil Mechanics, Chinese Academy of Sciences.

https://doi.org/10.1016/j.jrmge.2020.02.004

the recent years, few studies have adopted complex data acquisition systems to record pressure variation throughout the test for enhancing the accuracy in permeability measurement (Tonder and Jacobsz, 2017).

On the contrary, the conventional falling-head test setup involving a drop in water level at the inlet boundary, and by maintaining a constant water level at the outlet boundary, yields result with moderate accuracy (Singh and Gupta, 2000). However, these methods either suffer from inaccuracies due to the evaporation loss and/or demand expensive data acquisition systems. Further, quantification of variation in the head difference due to evaporation is impractical. The error associated with these scenarios can result in a significant variation in the measured coefficient of permeability. For instance, if the permeability test on a soil sample having 50 mm in diameter and 10 mm in thickness in a conventional falling-head setup with inlet tube diameter of 6 mm provides a head drop from 180 mm to 130 mm in 3 h, the coefficient of permeability would be 4.34×10^{-9} m/s. If 2 mL of water was evaporated from the inlet tube during the test, which is possible during the permeability test in an accelerated gravity environment, instead of the final inlet head of 130 mm, the observed head would be 78 mm resulting in a coefficient of permeability of 1.12×10^{-8} m/s. Given this, the development of a permeability setup that can overcome this lacuna is mandatory. In addition, when a geomaterial under consideration is to be evaluated for its suitability as a landfill liner, involving leachate as permeant liquid is inevitable. Considering the practical difficulty, researchers have resorted to simulated or synthetic leachate instead of actual leachate collected from an engineered landfill (Rowe et al., 2002; Badv and Omidi, 2007; Bradshaw and Benson, 2014; Mishra et al., 2015; Leme and Miguel, 2018).

The present study aimed to investigate the permeability behavior of biopolymer-modified SBMs from the perspective of landfill liner applications. A simple permeability apparatus that can be used in the geotechnical centrifuge, without any complex data acquisition system, was developed. Also, the permeability of the chosen biopolymer-modified SBMs was assessed as per ASTM D5084-16a (2016), using the flexible wall permeameter, to validate the results obtained from the proposed permeability apparatus. Further, the role of confinement in terms of changing volume of the sample by allowing and restraining its void ratio was assessed.

2. Materials and experimental investigations

The specimens used for this study were prepared by mixing guar gum and xanthan gum at different dry weight fractions with SBMs. Sodium bentonite of high purity supplied by the Versatile Specialty Mine Chem, Bhuj, India, was used for preparing various SBMs having different bentonite fractions in them. The X-ray diffractogram and other basic characteristics of selected bentonite reported in Fig. 1a and Table 1 confirm that the dominant mineral is montmorillonite. The chemical composition of the bentonite was assessed by employing X-ray fluorescence spectrometer, and the elemental composition in its oxide form is listed in Table 2.

Srikanth (2017) studied the effect of the grain size distribution of sand in SBM on its overall engineering performance and reported that fine-sand provides smaller coefficient of permeability compared to coarse-sand. Given this observation, Indian standard fine-sand (grade-III) was chosen for this study, and its physical and mineralogical characteristics are shown in Fig. 1b and Table 1.

Table 1
Physical properties of materials used in the study.

Material	Property	Unit	Value	Standard
Bentonite	Specific gravity		2.73	ASTM D5550-14 (2014)
	Liquid limit	%	750	ASTM D4318-17 (2017)
	Plastic limit	%	50	ASTM D4318-17 (2017)
	Plasticity index	%	700	ASTM D4318-17 (2017)
	Shrinkage limit	%	12	ASTM D427-04 (2004)
	Zeta potential	mV	−121	
	Organic content	%	0.428	ASTM D2974-14 (2014)
	Swell index	mL/(2 g)	43	ASTM D5890-11 (2011)
	pH value		7.8	ASTM D4972-18 (2018)
	Content of fine sand	%	0	
	Content of silt	%	0	
	Content of clay	%	100	
	Classification of soil		CH	ASTM D2487-17 (2017)
Fine-sand	Specific gravity		2.65	ASTM D5550-14 (2014)
	Effective size, D_{10}	mm	0.16	
	D_{30}	mm	0.23	
	D_{60}	mm	0.28	
	Uniformity coefficient, C_u		1.72	
	Coefficient of curvature, C_c		1.15	
	Maximum void ratio, e_{max}		0.9	ASTM D4253-16 (2016)
	Minimum void ratio, e_{min}		0.6	ASTM D4254-16 (2016)
	pH value		8	ASTM D4972-18 (2018)
	Content of fine sand	%	100	
	Content of silt	%	0	
	Content of clay	%	0	
	Classification of soil		SP	

Note: Fine sand size: ≤0.425 mm and >0.075 mm; silt size: ≤0.075 mm and >0.002 mm; clay size: ≤0.002 mm; D_{10}: The grain diameter corresponding to 10% passing; D_{30}: The grain diameter corresponding to 30% passing; D_{60}: The grain diameter corresponding to 60% passing.

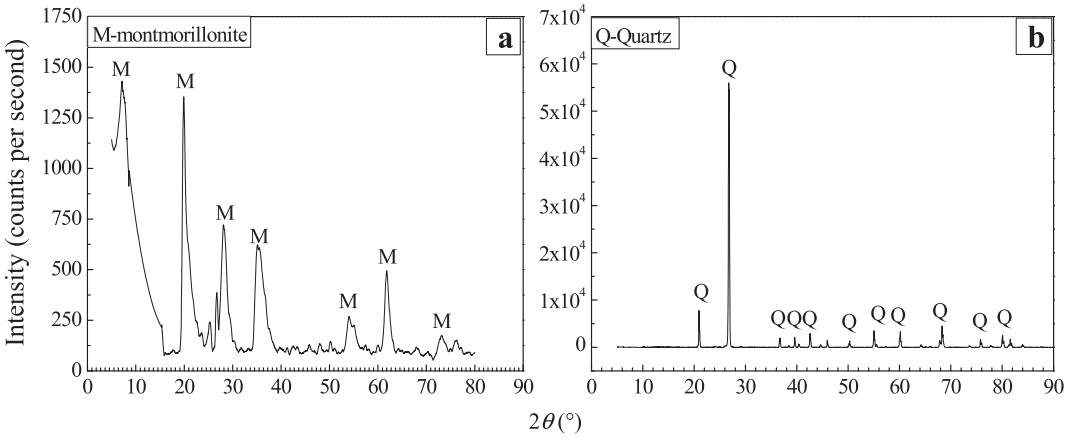

Fig. 1. X-ray diffractogram of (a) fine-sand and (b) bentonite.

Table 2
Chemical composition (%) of bentonite.

Na^{+}	Mg^{2+}	Al^{3+}	Si^{4+}	S^{6+}	K^{+}	Ca^{2+}	Sc^{3+}	Ti^{4+}	V^{5+}	Fe^{3+}	Zn^{2+}	O^{2-}
3.3	3.35	8.58	27.69	0.22	0.14	0.55	0.01	0.78	0.08	8.07	0.07	47.2

The fine-sand was mixed thoroughly with bentonite in a dry condition at various proportions by weight (25%, 45%, 65% and 85%). The geotechnical characteristics of the SBMs were determined as per relevant standards (ASTM D698-12, 2012; ASTM D4318-17, 2017), and the obtained results are reported in Table 3.

Anionic biopolymer xanthan gum and non-ionic biopolymer guar gum supplied by Sisco Research Laboratories, Bombay, India, were used as the soil stabilizers. As per the World Health Organization (WHO), the selected biopolymers are considered to be nontoxic, and hence, no dosage limits were prescribed for ingestion (WHO, 1975, 1987). Guar gum is derived from the seeds of *Cyamopsis tetragonoloba*, and the hydroxyl groups in its polymer chains help in forming hydrogen bonds. Xanthan gum, a branched polysaccharide produced by Xanthomonas bacteria, is commercially available since 1960. Xanthan gum has cellobiose as the monomer and the polymer side chains consisting of a trisaccharide were composed of D-mannose (β-1,4), D-glucuronic acid (β-1,2) and D-mannose, which is attached to alternate glucose residues in the backbone by α-1,3 linkages (Petri, 2015). Xanthan gum is a highly stable polysaccharide that is not easily degraded by the microorganisms presented in the soil (Cadmus et al., 1982). The viscosities of 2% guar gum and 3% xanthan gum solutions are more than 700 Pa s, and hence wet mixing of biopolymer beyond these concentrations with the soil becomes tedious (Chudzikowski, 1971; Chen et al., 2013). As the high viscosity brings down the workability, the maximum quantities of guar gum and xanthan gum to be added were restricted to 2% and 3% by weight of soil, respectively.

Biopolymers can be mixed with geomaterials using either wet-mixing or dry-mixing technique. In the wet-mixing procedure, initially, a solution of a biopolymer is prepared by mixing a known quantity of biopolymer with water, and then the solution is uniformly mixed with soil. In dry-mixing, soil and powdered biopolymer are mixed thoroughly in dry condition, and subsequently, water is added to it (Chang et al., 2015). When a biopolymer is added to water in the wet-mixing approach, the configuration of the biopolymer changes from coiled to an extended form (Theng, 2012). On the contrary, during dry-mixing, the coiled biopolymers in the constrained void spaces cannot access as many soil-solid surfaces as in the wet-mixing even after addition of water. Owing to the advantages of wet-mixing, the biopolymers in different fractions (0.5%, 1%, 1.5%, 2% and 0.5%, 1%, 2%, 3% for guar gum and xanthan gum, respectively) and SBMs were wet-mixed, to assess the engineering properties of the biopolymer-modified SBMs.

Table 3
Geotechnical characteristics of sand-bentonite mixtures.

Sand content (%)	Liquid limit (%)	Plastic limit (%)	Optimum moisture content (%)	Maximum dry unit weight (kN/m^3)
0	750	50	45	12
25	460	41	30	13.9
45	355	30	22.5	15.6
65	245	27	15.6	17.4
85	120	25	13.8	18.3

Based on the results of the standard Proctor compaction test, the weight of SBM and quantity of water required for preparing specimens having a known compaction state were calculated. A known quantity of biopolymer was added to the predetermined volume of deionized water and mixed thoroughly in an orbital shaker for 48 h, to ensure the proper dispersion of biopolymer in the suspension. The suspension thus prepared was mixed with SBM and allowed it to mature by storing it in an air-tight polyethylene bag.

Deionized water and strong synthetic leachate were selected for conducting the permeability experiments. Bradshaw and Benson (2014) analyzed data of more than 2000 landfill leachate samples and suggested the composition of real and synthetic leachates. Their analysis was primarily based on the ionic strength and relative abundance of monovalent and multivalent cations (RMD) presented in the leachate. Given this observation, the present study has considered synthetic leachate having the chemical composition as suggested by Bradshaw and Benson (2014), and the details are listed in Table 4.

For performing a flexible wall permeability test, the premixed SBM was placed in a mold and compacted to obtain a cylindrical specimen of 38 mm in diameter and 25 mm in height representing its optimum compaction state. The permeability of the specimen was measured following ASTM D5084-16a (2016). The initial portions of the curves of time versus volumes of the influent and effluent were found to exhibit slightly different slopes due to the progressive saturation of the sample. Hence, the segment in which the curves of time versus influent and effluent volumes have shown identical response is used for determining the coefficient of permeability of SBMs.

Since the flexible wall permeameter demands long testing periods to arrive at the coefficient of permeability, a modified-falling head permeameter setup is fabricated, as shown in Fig. 2, for assessing the permeability of SBMs using a geotechnical centrifuge. The permeability apparatus consists of a 50 mm diameter Perspex tube fixed on a rigid platform, which allows the water to move out through an opening connected to a 10 mm diameter graduated tube. The soil sample is kept at the bottom of the Perspex tube, which, in turn, is sandwiched between porous stones. To avoid the change in volume of the specimen due to swelling, the movement of the upper porous disc is restrained using a spacer rod. Water was filled in the 10 mm diameter graduated tube to impose a known hydraulic head, and the entire setup was subjected to centrifugation, allowing permeant liquid to flow through the soil in an upward direction. This arrangement avoids the preferential flow of permeant liquid through an unnoticeable annular space between the sample and the inner circumference of the Perspex tube as well as through the micro-cracks which might have formed during the sample preparation. The percolate passing through the specimen was allowed to accumulate on its top (i.e. within the large Perspex

Table 4
Chemical properties of permeant liquid.

Permeant liquid	Cation concentration (mmol/L)				Ionic strength (mmol/L)	RMD ((mol/L)$^{0.5}$)	pH value	Electrical conductivity (mS/m)
	Na^{+}	K^{+}	Mg^{2+}	Ca^{2+}				
Deionized water	0	0	0	0	0	0	6.9	5
Synthetic leachate	33.1	4.9	18.7	13.5	83.5	0.212	7.1	950

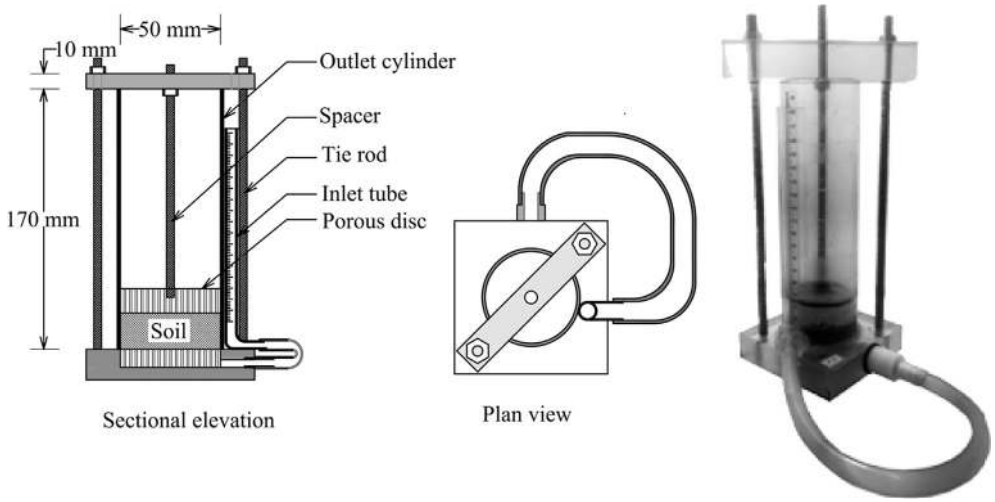

Fig. 2. Schematic and pictorial view of proposed falling-head permeameter.

tube of 50 mm in diameter). Before measurement of the coefficient of permeability of the sample, a minimum of three pore volumes of permeant liquid was allowed to pass through it for ensuring its complete saturation.

While constructing the compacted clay liners as a part of the cover liner system of an uncontrolled waste dumps or as an engineered intermediate landfill cover, these liners are not subjected to surcharge loads. To simulate these field scenarios, the permeability tests were conducted by allowing the change in volume of the specimen in an upward direction. The permeant liquid was allowed to flow through the sample until the volume change ceases before measuring its permeability. For simulating the 500 mm thick liner in the field, the specimen of 10 mm in thickness was subjected to accelerated gravity of 50 times the acceleration of gravity on the surface of the earth (Taylor, 2005). A similar procedure was followed for simulating the permeation of leachate through the liner by considering the synthetic leachate as the permeant liquid.

Since the hydraulic boundary conditions (i.e. water levels in the proposed setup) at the inlet and outlet of the specimen are continuously varying during the falling-head test, the formulation of a mathematical expression for determining the coefficient of permeability is essential and the derivation of the same is explained, as shown in Fig. 3.

Let the cross-sectional area of graduated inlet tube be a, and the cross-sectional area of specimen (i.e. large Perspex cylinder) be A. In a given test duration dt, the water level was reduced by dh_1 in the graduated tube and increased by dh_2 in the large Perspex cylinder, causing a head difference to reduce from h_1 to h_2, as shown in Fig. 3.

When the soil sample is completely saturated, the decrease in the volume of water in the smaller tube should be equal to an increase in the volume of water in the larger cylinder as given below:

$$a\mathrm{d}h_1 = A\mathrm{d}h_2 \tag{1}$$

The head difference caused due to flow in time dt is

$$\mathrm{d}h = h_1 - h_2 = \mathrm{d}h_1 + \mathrm{d}h_2 \tag{2}$$

Substituting Eq. (1) into Eq. (2) results in the following relationship:

$$\mathrm{d}h_1 = \frac{A}{A+a}\mathrm{d}h \tag{3}$$

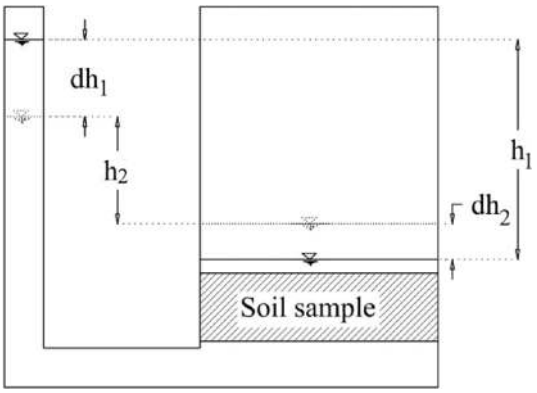

Fig. 3. Variation of the hydraulic head during the falling head permeability test. dh_1 and dh_2 are the water level variations in graduated inlet and outlet tubes in the permeameter, respectively; and h_1 and h_2 are the initial and final head differences, respectively.

In general, the governing equation for flow through porous media can be expressed as

$$-\frac{\partial p}{\partial x} = \frac{1}{k}\mu v_\mathrm{f} + \beta\rho v_\mathrm{f}^2 \tag{4}$$

where p is the pressure, x is the length of the porous media, k is the intrinsic coefficient of permeability, μ is the dynamic viscosity of permeant liquid, v_f is the velocity of flow, ρ is the fluid density, and β is the Forchheimer coefficient (Bear, 1972; Hellström and Lundström, 2006; Sobieski and Trykozko, 2014). When the seepage velocity is low, and the corresponding Reynolds number, Re, is less than unity, Eq. (4) reduces to Darcy's law. Incidentally, the seepage velocity through the geomaterials considered in this study is found to be very small, and hence, Darcy law can be used to represent the flow of permeant liquid in these materials. According to Darcy law, the volume of water flowing through the sample in time dt is

$$a\mathrm{d}h_1 = kiA_\mathrm{s}\mathrm{d}t = k\frac{h}{L}A_\mathrm{s}\mathrm{d}t \tag{5}$$

where A_s is the cross-sectional area of soil specimen, L is the length of soil specimen, and i is the hydraulic gradient.

Substituting Eq. (3) into Eq. (5) yields

$$a\left(\frac{A}{A+a}\right)\mathrm{d}h = k\frac{h}{L}A_s\mathrm{d}t \tag{6}$$

If the flow through the soil sample from time t_1 to t_2 causes a head difference to fall from h_1 to h_2, it can be represented as

$$\int_{h_2}^{h_1}\frac{\mathrm{d}h}{h} = \int_{t_2}^{t_1} k\frac{(A+a)A_s}{A}\frac{1}{aL}\mathrm{d}t \tag{7}$$

Integrating and rearranging the terms results in the expression for the coefficient of permeability as

$$k = \frac{2.303aL}{A_s\Delta t\left(1+\frac{a}{A}\right)}\log_{10}\frac{h_1}{h_2} \tag{8}$$

In each permeability test, the angular velocity in terms of rotations per minute (RPM) was calculated to obtain imposed gravitational field (i.e. *Ng* value, where *N* is a multiplying factor, and *g* is the acceleration due to gravity), and the permeameters containing soil specimens were centrifuged for a definite period. The weight of permeameter with the sample and permeant liquid, and the fluid level in the inlet and outlet tubes were noted before and after the test. The cross-sectional areas, test duration, and angular velocity were recorded. For each sample, experiments were conducted in duplicate and the average value of the coefficient of permeability was reported.

Evaporation from the inlet and outlet occurs with the permeation during the centrifugation. To quantify the water level drop due to evaporation, a setup having four different diameter tubes is fabricated, as shown in Fig. 4 and subjected to centrifugation along with permeameters. The loss of water level in the tubes was determined and it was found that the evaporation is proportional to D^n, where D is the diameter of the tube and n is a constant. Hence, mass loss, w_t, from the graduated tube of diameter d in time Δt can be written as follows:

$$w_t = k_e d^n \Delta t \tag{9}$$

where k_e is the proportionality constant.

Similarly, mass loss, w_c, due to evaporation from the large Perspex tube of diameter D can be written as

$$w_c = k_e D^n \Delta t \tag{10}$$

If the total mass loss which can be directly measured is w, the constant of proportionality can be determined as

$$k_e = \frac{w}{\Delta t\left(d^n + D^n\right)} \tag{11}$$

The level drop from tube and containers can be determined as $wd^n/[\pi d^2(d^n+D^n)]$ and $wD^n/[\pi D^2(d^n+D^n)]$, respectively. The final head difference h_2' after incorporating the evaporation correction becomes

$$h_2' = h_2 - \left[\frac{w}{\pi\left(d^n+D^n\right)}\left(\frac{D^n}{D^2}-\frac{d^n}{d^2}\right)\right] \tag{12}$$

The coefficient of permeability determined using the centrifuge permeability test at *Ng* condition will be *N* times that of the permeability at the 1*g* condition. Hence, coefficient of permeability from centrifuge permeability test can be written as

$$k = \frac{2.303aL}{NA_s\Delta t\left(1+\frac{a}{A}\right)}\log_{10}\frac{h_1}{h_2'} \tag{13}$$

To understand the primary reason behind the change in permeability of biopolymer-modified SBMs with sand and biopolymer contents, the morphological study was conducted with the help of a scanning electron microscope (SEM). The fabric variation of bentonite with the addition of biopolymers was imaged and investigated.

3. Results and discussion

The results of evaporation from the tubes having different diameters are shown in Fig. 5. The analysis of evaporation data provides the n value used in Eqs. (9)-(12) as 1.8, which matches with the value reported in the literature (Hisatake et al., 1993).

Fig. 6 shows the results of the permeability test conducted on SBMs having different sand contents. The results from the flexible wall permeability tests under the constant-head and centrifuge permeability tests in 50*g*, 100*g*, and 150*g* conditions under variable-head corroborate each other, demonstrating the efficacy of the proposed test methodology. The trend shows a sudden variation in the permeability only when the sand content exceeds 65% in the SBMs. Hence, the value 65% can be considered as a threshold, which causes a variation in the soil structure. The coefficient of permeability of pure bentonite is moderately less than that of all SBMs considered in this study. Based on these results, pure bentonite and SBM with 65% sand content (SBM_{65}) were considered for assessing

Fig. 4. Test setup to study the variation in evaporation rate with tube diameter.

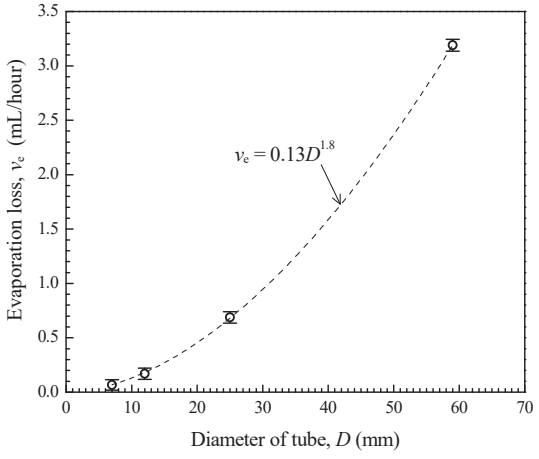

Fig. 5. Variation in evaporation rate with the diameter of tubes.

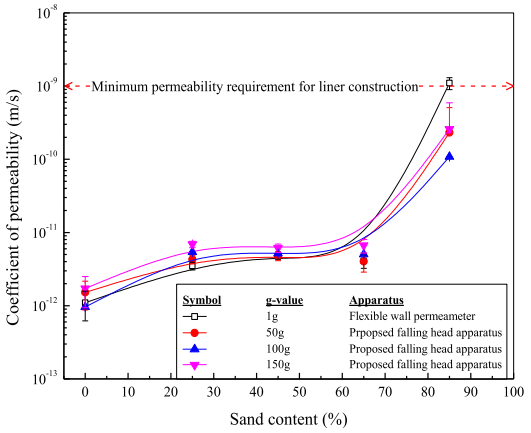

Fig. 6. Variations in the coefficient of permeability of sand-bentonite mixtures with sand content.

the influence of biopolymer amendment on their permeability characteristics.

Fig. 7 shows the variations of coefficient of permeability of SBM_{65} and pure bentonite with the biopolymer content. The difference in permeability when volume change is restricted (confined) and allowed (unconfined) is also depicted. Fig. 8 shows the variations of the coefficient of permeability when the permeant liquid is synthetic leachate. It can be observed from Figs. 7 and 8 that the coefficient of permeability of geomaterials considered in this study is greater when tested by allowing the volume change of the sample. For comparison, both flexible wall and confined falling-head tests are required to perform; however, the unconfined falling-head tests represent the field scenario of cover liners, and hence results from these tests shall be used in the design of liners. An increase in biopolymer content causes an increased permeability, which is contradicting with the permeation behavior of biopolymer-modified noncohesive and nonexpansive soils reported in the literature. Results from the tests using synthetic leachate also indicate higher permeability values. Though the coefficient of permeability of biopolymer-modified SBMs is higher than that of untreated SBMs, the coefficients of permeability of modified-SBMs are less than threshold of 1×10^{-9} m/s, recommended by various regulatory authorities (CJJ113, 2007; CPHEEO, 2016). Hence, biopolymer modification can be recognized as an effective stabilization strategy, considering its superior performance in terms of crack resistance and strength, as highlighted in the literature (Biju and Arnepalli, 2019).

3.1. Variation of permeability with sand content

It can be observed from Fig. 7 that the permeability of SBM increases with an increase in sand content. In addition to the formation of preferable paths through the sand-bentonite interface, the change in the fabric also plays a crucial role in the permeability increase. The geomaterial initially in cohesive structure moves towards the coarse-grained skeletal structure with an increase in sand content. Previous studies have concluded that geomaterial in cohesive structure performs better as hydraulic barriers (Kenney et al., 1992; Proia et al., 2016). On the contrary, for the geomaterials to be in coarse-grained structure, the sand skeletal void volume, e_{sv}, should be higher than the volume occupied by bentonite. With an increase in sand content, e_{sv} increases and bentonite volume decreases. When the sand content reaches 85%, the fabric changes from fine-grained to coarse-grained skeletal structure, providing easier paths for permeant liquid to move through it. This results in a considerable increase in the coefficient of permeability. Though the volume of hydrated bentonite volume is sufficient to fill all the voids corresponding to e_{sv}, nonuniform distribution of bentonite and sand may create preferential paths, as shown in Fig. 9. The SBM having a sand content up to 65% yields clay matrix structure even when the mixtures are air-dried. This is due to the fact that the volume of bentonite at its shrinkage limit is sufficient to fill the sand skeletal void volume. Consequently, the increase in sand content beyond this threshold leads to an increase in coefficient of permeability, as depicted in Fig. 6.

3.2. Variation of permeability with biopolymer content

Figs. 7 and 8 show an increase in permeability with addition of biopolymers. The flow of permeant liquid through a compacted specimen will be through inter- and intra-aggregate flow paths, as shown in Fig. 10, and the inter-aggregate flow paths will be contributing much to the coefficient of permeability (Olsen, 1962; Scholes et al., 2007; Bayesteh and Mirghasemi, 2015). Water

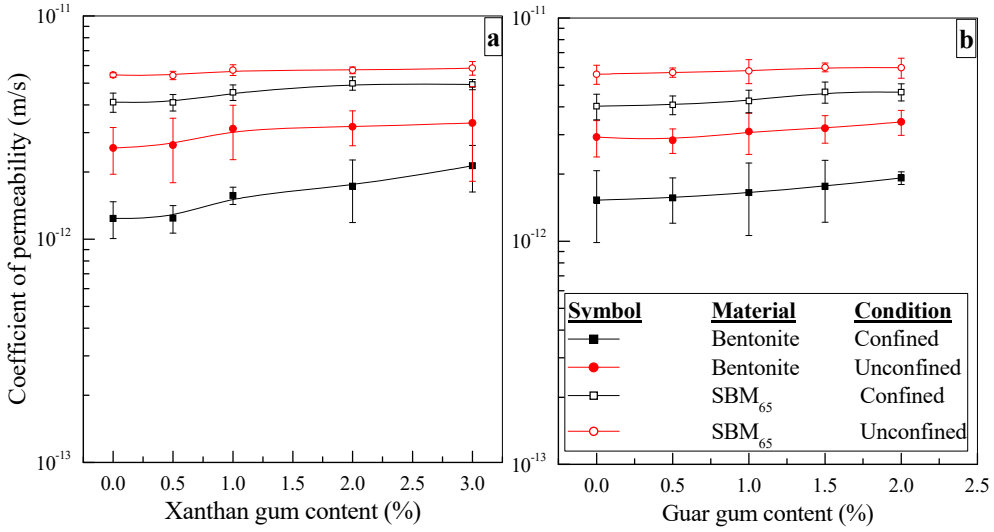

Fig. 7. Variations in the coefficient of permeability of bentonite and sand-bentonite mixture determined using deionized water as permeant liquid, amended with (a) xanthan gum and (b) guar gum.

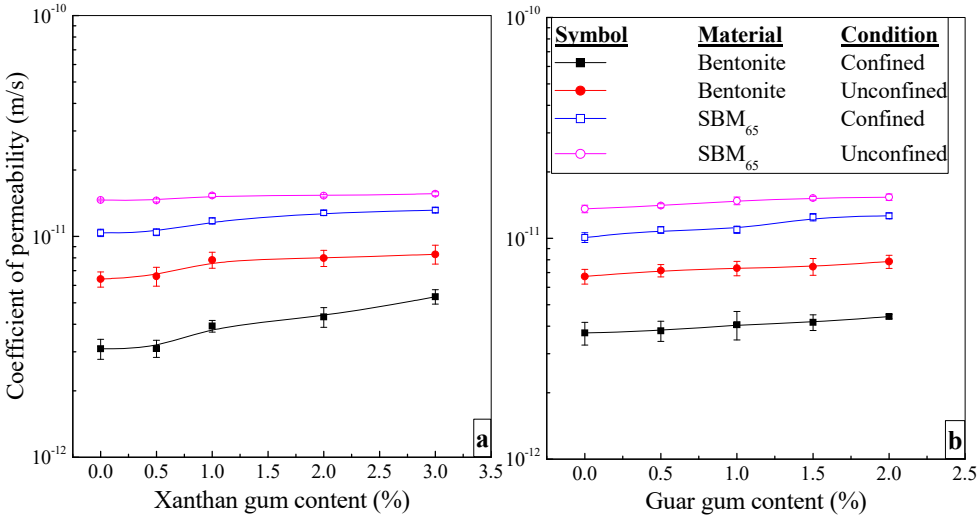

Fig. 8. Variations in the coefficient of permeability of bentonite and sand-bentonite mixture determined using synthetic leachate as permeant liquid, amended with (a) xanthan gum and (b) guar gum.

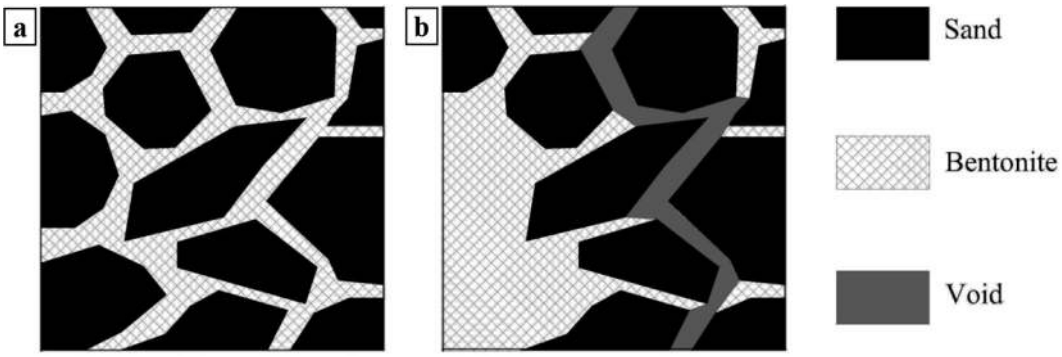

Fig. 9. Schematic indicating the formation of preferential flow paths (a) from uniform distribution of sand and bentonite and (b) from nonuniform distribution of sand and bentonite.

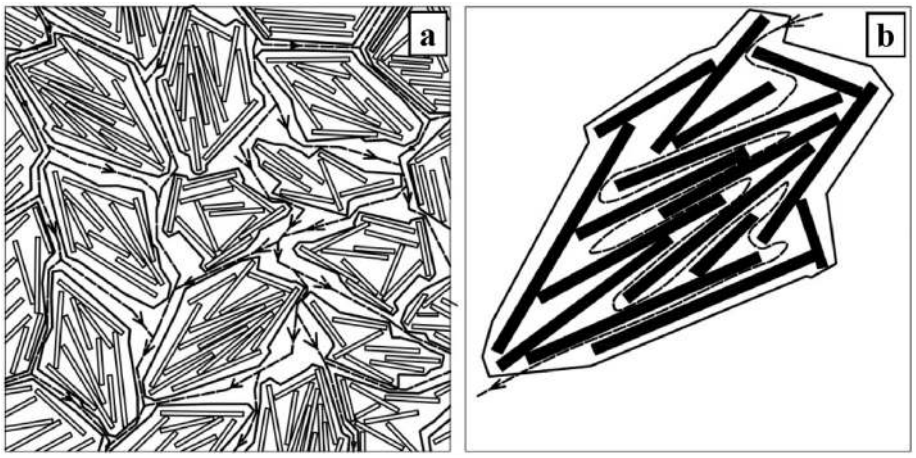

Fig. 10. Flow paths in compacted clay specimen through (a) inter-aggregate pores and (b) intra-aggregate pores.

molecules firmly attached around the clay particles inside aggregate will create negligibly small effective flow paths allowing flow only through the inter-aggregate paths. Thus the size and formation of aggregates or packets in clays considerably influence permeability (Benson and Daniel, 1990).

The addition of biopolymers causes aggregation of clay particles by binding them together, forming higher sized aggregates (Nugent, 2011). When a biopolymer is added to the soil, it forms a thin coating over the aggregates through secondary bonds. The polar components in the biopolymer may participate in the

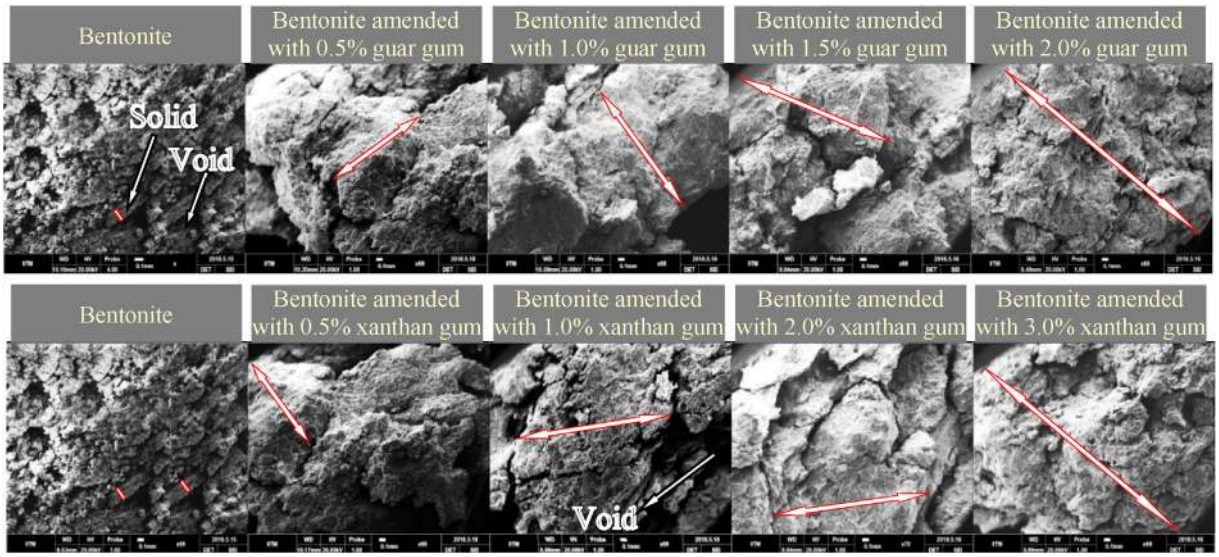

Fig. 11. Scanning electron microscope images of biopolymer-modified bentonite.

interaction with the charged surfaces of the soil, which in turn enhances the adhesion. As a result, the ionic, hydrogen or van der Waals bonds lead to enwrapment of the soil aggregates and formation of larger aggregates. The SEM images at 68 times of magnification shown in Fig. 11 helps in explaining how the aggregate size changes with an increase in biopolymer content. Smaller aggregate size and pore size can be observed in the SEM image of untreated bentonite. In the next image with 0.5% biopolymer, these aggregates combine together to form a much larger one causing larger voids. The aggregate size and void size progress with increases in both guar gum and xanthan gum addition, as indicated in Fig. 11 using double-headed arrows. The increased aggregation leads to larger inter-aggregate flow paths resulting in higher permeability.

The observed increase in permeability with addition of biopolymers is well within one order of magnitude, as presented in Figs. 7 and 8. If the sole reason for the change in permeability is the change in aggregate size, the variation should have been higher than the observed value. Liu et al. (2017) described the mechanisms of soil stabilization by polymers as a collective process of filling the void volume, enwrapping, and physicochemical interaction. The hydrogel formed with the biopolymers existing in the pore spaces will cause a reduction in the flow. The interactions between the soil and biopolymer are predominantly physical in nature. Majority of the physisorption interactions exhibit reversibility; however, the probability of desorption of the polymer from the soil is restrained by the octopus effect of the biopolymer (Theng, 2012). Even after the flow of many pore volumes of water or leachate through the soil, the octopus effect holds the biopolymers in position. Thus a combined effect of the widening of the flow paths, filling a portion of the voids and the octopus effect controls the coefficient of permeability.

3.3. Role of confinement

The flow through the selected material under confined conditions is less than that under unconfinements. When the material is used as an intermediate cover liner, no significant surcharge load acts on it to arrest the volume change. This scenario was simulated by performing the tests under unconfined conditions. The permeability test under an accelerated gravity environment conducted to simulate a field liner of 500 mm thick provided higher permeability, as seen in Figs. 7 and 8. As the flow occurs through the inter-aggregate voids, it tries to push away the aggregates, creating larger flow channels; the flow will be through these enlarged channels providing higher permeability. However, in the field, the possibility of such a high potential head, which can cause the creation of easier paths through pushing away the particles, is rare. Nevertheless, being on the conservative side, it is advisable to use the permeability values obtained from the unrestrained test.

3.4. Role of leachate

The lower coefficient of permeability of SBM obtained while tested with deionized water is mainly attributed to the reduction in the size of the effective flow channels, which in turn is influenced by the diffused double-layer of montmorillonite mineral presented in it (Mesri and Olson, 1971). The increase in cation concentration (leachate as a permeant liquid) results in contraction of diffused-double layer and causes broader flow paths, which in turn alters the coefficient of permeability. For instance, the k value of SBM_{65} is changed from 10^{-11} m/s to 10^{-10} m/s, when the permeant liquid is synthetic leachate instead of deionized water. Since the concentration of cations in synthetic leachate is significant, the permeability increases when tested under both confined and unconfined conditions. As the flow of leachate through an intermediate liner is evident, the permeability values obtained using SL are advisable for design of such liners.

4. Conclusions

This study analyzed the effect of the biopolymer amendment on permeability characteristics of SBMs. To overcome the limitation of the longer duration of test associated with flexible wall permeameter, a modified-falling head permeameter apparatus, which considers the evaporation aspect, is presented. The proposed apparatus was used to assess the variation in permeability of biopolymer-modified SBMs by allowing and restraining volume change of the specimen, under an accelerated gravity environment. The permeability of a compacted material subjected to volume change is higher compared to that of restrained condition. The variation in permeability when the permeant liquid changed from

deionized water to leachate was also presented. The results inferred that SBMs with sand content up to 65% can be used as liner material for the construction of intermediate compacted clay liners.

Further, it was established that the biopolymer amendment had induced aggregation of clay platelets, which in turn created wider effective flow paths. The change of permeant liquid from deionized water to leachate resulted in the contraction of the diffused double-layer on the clay surface. Flow-through the soil in an unrestrained condition allowed the aggregates to move apart by enabling the permeant liquid to pass through the increased pore spaces. The synergetic influence of the factors mentioned above is found to be responsible for an increase in the permeability of biopolymer-modified SBMs. However, even in the most critical condition, where the flow of synthetic leachate through SBM with 65% sand content under an unrestrained condition, the coefficient of permeability of the modified-SBM was found to be less than the minimum threshold advocated by regulatory guidelines (i.e. $\leq 1 \times 10^{-11}$ m/s). Based on this observation, it can be concluded that the proposed environmental-friendly stabilization technique can be accepted to improve the overall engineering properties of geomaterials.

Declaration of competing interest

The authors wish to confirm that there are no known conflicts of interest associated with this publication and there has been no significant financial support for this work that could have influenced its outcome.

References

Abdi MR, Parsapajouh A, Arjomand MA. Effects of random fiber inclusion on consolidation, hydraulic, conductivity, swelling, shrinkage limit and desiccation cracking of clays. International Journal of Civil Engineering 2008;6(4):284–92.

Acharya R, Pedarla A, Bheemasetti TV, Puppala AJ. Assessment of guar gum biopolymer treatment toward mitigation of desiccation cracking on slopes built with expansive soils. Transportation Research Record: Journal of the Transportation Research Board 2017;2657(1):78–88.

Adaska WS. Soil-cement liners. In: Johnson I, Frobel RK, Cavalli NJ, Pettersson CB, editors. Hydraulic barriers in soil and rock. ASTM STP 874. American Philadelphia, USA: Society for Testing and Materials (ASTM); 1985. p. 299–313.

Anderson C, Sivakumar V, Black JA. Measurement of permeability using a bench-top centrifuge. Géotechnique 2015;65(1):12–22.

ASTM D427-04. Standard test method for shrinkage factors of soils by the mercury method. West Conshohocken, USA: ASTM International; 2004.

ASTM D4318-17. Standard test methods for liquid limit, plastic limit, and plasticity index of soils. West Conshohocken, USA: ASTM International; 2017.

ASTM D698-12. Standard test methods for laboratory compaction characteristics of soil using standard effort. West Conshohocken, USA: ASTM International; 2012.

ASTM D2487-17. Standard practice for classification of soils for engineering purposes (Unified Soil Classification System). West Conshohocken, USA: ASTM International; 2017.

ASTM D2974-14. Standard test methods for moisture, ash, and organic matter of peat and other organic soils. West Conshohocken, USA: ASTM International; 2014.

ASTM D4253-16. Standard test methods for maximum index density and unit weight of soils using a vibratory table. West Conshohocken, USA: ASTM International; 2016.

ASTM D4254-16. Standard test methods for minimum index density and unit weight of soils and calculation of relative density. West Conshohocken, USA: ASTM International; 2016.

ASTM D4972-18. Standard test methods for pH of soils. West Conshohocken, USA: ASTM International; 2018.

ASTM D5084-16a. Standard test methods for measurement of hydraulic conductivity of saturated porous materials using a flexible wall permeameter. West Conshohocken, USA: ASTM International; 2016.

ASTM D5550-14. Standard test method for specific gravity of soil solids by gas pycnometer. West Conshohocken, USA: ASTM International; 2014.

ASTM D5890-11. Standard test method for swell index of clay mineral component of geosynthetic clay liners. West Conshohocken, USA: ASTM International; 2011.

Ayeldeen M, Negm A, El-Sawwaf M, Kitazume M. Enhancing mechanical behaviors of collapsible soil using two biopolymers. Journal of Rock Mechanics and Geotechnical Engineering 2017;9(2):329–39.

Badv K, Omidi A. Effect of synthetic leachate on the hydraulic conductivity of clayey soil in Urmia City landfill site. Iranian Journal of Science and Technology 2007;31:535–45.

Bayesteh H, Mirghasemi AA. Numerical simulation of porosity and tortuosity effect on the permeability in clay: microstructural approach. Soils and Foundations 2015;55(5):1158–70.

Bear J. Dynamics of fluids in porous media. Elsevier; 1972.

Benson CH, Daniel DE. Influence of clods on hydraulic conductivity of compacted clay. Journal of Geotechnical Engineering 1990;116(8):1231–48.

Biju MS, Arnepalli DN. Biopolymer-modified soil: prospects of a promising green technology. In: Stalin VK, Muttharam M, editors. Geotechnical characterisation and geoenvironmental engineering. 1st ed. Springer; 2019. p. 163–9.

Bouazza A, Gates WP, Ranjith PG. Hydraulic conductivity of biopolymer-treated silty sand. Géotechnique 2009;59(1):71–2.

Bradshaw SL, Benson CH. Effect of municipal solid waste leachate on hydraulic conductivity and exchange complex of geosynthetic clay liners. Journal of Geotechnical and Geoenvironmental Engineering 2014;140(4):04013038. https://doi.org/10.1061/(ASCE)GT.1943-5606.0001050.

Cabalar AF, Wiszniewski M, Skutnik Z. Effects of xanthan gum biopolymer on the permeability, odometer, unconfined compressive and triaxial shear behavior of a sand. Soil Mechanics and Foundation Engineering 2017;54(5):356–61.

Cadmus MC, Jackson LK, Burton KA, Plattner RD, Slodki ME. Biodegradation of xanthan gum by bacillus. Applied and Environmental Microbiology 1982;44(1):5–11.

Chaduvula U, Viswanadham BVS, Kodikara J. A study on desiccation cracking behavior of polyester fiber-reinforced expansive clay. Applied Clay Science 2017;142:163–72.

Chang I, Im J, Cho GC. Soil-hydraulic conductivity control via a biopolymer treatment-induced bio-clogging effect. In: Proceedings of the geotechnical and structural engineering congress, Phoenix, Arizona; 2016. p. 1006–15.

Chang I, Im J, Prasidhi AK, Cho GC. Effects of xanthan gum biopolymer on soil strengthening. Construction and Building Materials 2015;74(15):65–72.

Chen R, Zhang L, Budhu M. Biopolymer stabilization of mine tailings. Journal of Geotechnical and Geoenvironmental Engineering 2013;139:1802–7.

Chudzikowski RJ. Guar gum and its applications. Journal of the Society of Cosmetic Chemists 1971;60(10):43–60.

CJJ113. Technical code for municipal solid waste sanitary landfill. Beijing, China: China Architecture and Building Press; 2007 (in Chinese).

CPHEEO. Municipal solid waste management manual: Part-II. New Delhi, India: Ministry of Urban Development, Government of India; 2016.

Dehghan H, Tabarsa A, Latifi N, Bagheri Y. Use of xanthan and guar gums in soil strengthening. Clean Technologies and Environmental Policy 2018;21(1):155–65.

Gueddouda MK, Goual I, Benabed B, Taibi S, Aboubekr N. Hydraulic properties of dune sandebentonite mixtures of insulation barriers for hazardous waste facilities. Journal of Rock Mechanics and Geotechnical Engineering 2016;8(4):541–50.

Hellström JGI, Lundström TS. Flow through porous media at moderate Reynolds number. In: Proceedings of the international scientific colloquium on modelling for material processing, riga; 2006. p. 129–34.

Hisatake K, Tanaka S, Aizawa Y. Evaporation rate of water in a vessel. Journal of Applied Physics 1993;73(11):7395–401.

Ikeagwuani CC, Nwonu DC. Emerging trends in expansive soil stabilisation: a review. Journal of Rock Mechanics and Geotechnical Engineering 2019;11(2):423–40.

Kenney TC, van Veen WA, Swallow MA, Sungaila MA. Hydraulic conductivity of compacted bentonite–sand mixtures. Canadian Geotechnical Journal 1992;29(3):364–74.

Khachatoorian R, Petrisor IG, Kwan CC, Yen TF. Biopolymer plugging effect: laboratory-pressurized pumping flow studies. Journal of Petroleum Science and Engineering 2003;38(1–2):13–21.

Latifi N, Horpibulsuk S, Meehan CL, Abd Majid MZ, Tahir MM, Mohamad ET. Improvement of problematic soils with biopolymer-an environmentally friendly soil stabilizer. Journal of Materials in Civil Engineering 2017;29(2):04016204. https://doi.org/10.1061/(ASCE)MT.1943-5533.0001706.

Leme MADG, Miguel MG. Permeability and retention to water and leachate of a compacted soil used as liner. Water, Air, and Soil Pollution 2018;229(374):1–19.

Liu J, Wang Y, Lu Y, Feng Q, Zhang F, Qi C, Wei J, Kanungo DP. Effect of polyvinyl acetate stabilization on the swelling-shrinkage properties of expansive soil. International Journal of Polymer Science 2017. https://doi.org/10.1155/2017/8128020. Article ID 8128020.

Maher M, Ho Y. Mechanical properties of kaolinite/fiber soil composite. Journal of Geotechnical Engineering 1994;120(8):1381–93.

Mesri G, Olson RE. Mechanisms controlling the permeability of clays. Clays and Clay Minerals 1971;19(3):151–8.

Mishra AK, Dutta J, Chingtham R. A study on the behavior of the compacted bentonite in the presence of salt solutions. International Journal of Geotechnical Engineering 2015;9(4):354–62.

Mukherjee K, Mishra AK. Performance enhancement of sand-bentonite mixture due to addition of fiber and geosynthetic clay liner. International Journal of Geotechnical Engineering 2017;11(2):1–7.

Nugent RA. The effect of exopolymers on the compressibility and shear strength of kaolinite. PhD Thesis. Louisiana, USA: Louisiana State University; 2011.

Olsen HW. Hydraulic flow through saturated clays. In: Proceedings of the 9th national conference on clays and clay minerals. Purdue University; 1962. p. 131–61.

Petri DFS. Xanthan gum: a versatile biopolymer for biomedical and technological applications. Journal of Applied Polymer Science 2015;132(23):1–17.
Proia R, Croce P, Modoni G. Experimental investigation of compacted sand-bentonite mixtures. Procedia Engineering 2016;158:51–6.
Rowe RK, VanGulck JF, Millward SC. Biologically induced clogging of a granular medium permeated with synthetic leachate. Journal of Environmental Engineering and Science 2002;1(2):135–56.
Scholes ON, Clayton SA, Hoadley AFA, Tiu C. Permeability anisotropy due to consolidation of compressible porous media. Transport in Porous Media 2007;68(3):365–87.
Singh DN, Gupta AK. Modelling hydraulic conductivity in a small centrifuge. Canadian Geotechnical Journal 2000;37(5):1150–5.
Singh DN, Kuriyan SJ. Estimation of hydraulic conductivity of unsaturated soils using a geotechnical centrifuge. Canadian Geotechnical Journal 2002;39(3):684–94.
Sobieski W, Trykozko A. Darcy's and Forchheimer's laws in practice. Part 1. The experiment. Technical Sciences 2014;17(4):321–35.
Sobti J, Singh SK. Techno-economic analysis for barrier materials in landfills. International Journal of Geotechnical Engineering 2017;11(5):467–78.
Srikanth V. Engineering behaviour of sand-bentonite mixtures and the influence of particle size of sand. PhD Thesis. Guwahati, India: Indian Institute of Technology; 2017.
Taylor RN. Geotechnical centrifuge technology. 1st ed. Taylor and Francis; 2005.
Theng BKG. Formation and properties of clay-polymer complexes. 2nd ed. Elsevier; 2012.
Thyagaraj T, Soujanya D. Polypropylene fiber reinforced bentonite for waste containment barriers. Applied Clay Science 2017;142:153–62.
Timms WA, Crane R, Anderson DJ. Accelerated gravity testing of aquitard core permeability and implications at formation and regional scale. Hydrology and Earth System Sciences 2016;20(1):39–54.
Tonder V, Jacobsz SW. Seepage column hydraulic conductivity tests in the geotechnical centrifuge. Journal of the South African Institution of Civil Engineering 2017;59(3):16–24.
WHO. Toxicological evaluation of some food colours, thickening agents, and certain other substances. In: Food additives series No. 8. World Health Organization (WHO); 1975.
WHO. Toxicological evaluation of certain food additives and contaminants. In: Food additives series No. 21. World Health Organization (WHO); 1987.

Dali Naidu Arnepalli obtained his BTech degree in Civil Engineering from Jawaharlal Nehru Technological University, Kakinada, India, in 2000, and his MTech and PhD degrees in Geotechnical Engineering from Indian Institute of Technology (IIT) Bombay, Powai, India, in 2002 and 2006, respectively. Dr. Arnepalli is a faculty member of the Department of Civil Engineering at the IIT Madras, Chennai, since December 2008. Before joining IIT Madras, he was associated with Prof. R. Kerry Rowe's research group at Geo-Engineering Centre, Queen's University, Ontario, Canada, for three years. Dr. Arnepalli's research group has developed a state-of-the-art Geoenvironmental Engineering Research Laboratory. His research interests include stabilization of geomaterials using biological processes and traditional methods, design of barrier systems and buffer materials for hazardous waste disposal, and geological sequestration of greenhouse gases.